



Effects of Continuous Printing on Fused Deposition-Modeled One-Way Large-Sized Parts

Ying-Guo Zhou and Xiao Huang

Submitted: 11 October 2020 / Revised: 24 February 2021 / Accepted: 4 March 2021 / Published online: 29 March 2021

One of the shortcomings of fused deposition modeling (FDM), a common and widely used additive manufacturing or 3D printing technique, is the limited size of the manufactured parts. Separately printing and gluing the parts is a common solution. In this study, a method of continuous printing for manufacturing one-way large-sized parts was proposed. Using the proposed method, FDM samples were fabricated with different interval times and linking-up locations. The mechanical properties, fracture behavior, and morphological structure were carefully investigated and compared with those obtained by conventional FDM and separately printing/gluing the parts. The results show that continuous printing helps to improve the mechanical properties of one-way large-sized FDM parts. After the interval time and linking-up location are optimized, the FDM parts have good mechanical properties, fracture behavior, and morphology. Thus, the proposed method is feasible and efficient for the continuous printing of one-way large-sized parts.

Keywords continuous printing, fused deposition modeling, interval time, linking-up location, one-way large-sized parts

1. Introduction

Fused deposition modeling (FDM) (Ref 1) is an extrusion-based rapid prototyping (RP) or additive manufacturing (AM) technique that has been developing at a fast pace and is widely used in electronic, electrical, telecommunications, tissue engineering, and automotive fields for both industrial production and personal consumption (Ref 2, 3). In a basic FDM process (Fig. 1), a polymer feedstock filament is drawn from a spool by drive wheels, heated to a melt state using a liquefier head, and then extruded through a nozzle (printing head) to deposit layer by layer on a temperature-controlled printer table. To directly fabricate 3D parts from a computer-aided design (CAD) model, the nozzle (or printing head) is generally computer controlled to move in the X and Y directions, while the printer table moves in the Z direction as required. After more than 30 years of development since 1988, FDM processes now enable the user to fabricate parts that range from a hollow to a fully solid structure with varying processing materials, shapes, sizes, and mechanical properties. Therefore, FDM has received considerable attention in academia and industry, and a series of studies have been reported on FDM materials (Ref 2-5), processes (Ref

6-8), part quality (Ref 9-11), equipment (Ref 12), mechanical properties (Ref 13-18), numerical simulation technology (Ref 19-22), and applications (Ref 23-27).

A restriction of the FDM process is the limited size of the fabricated parts. Considering the precision of the product and the convenience of the manufacturing process, the frames of an FDM machine are generally not too large. A deposition volume of $914 \times 609 \times 914 \text{ mm}^3$ is reported to be the maximum that can be manufactured by a commercially available FDM machine, e.g., the Fortus 900 mc (Ref 28). It must be noted that although the size of FDM machine can be larger, it is always limited. If the length of an FDM part exceeds the limitation of the size, using the existing FDM machine to manufacture the part in one step is difficult even though the width and height of the part are not particularly large. This type of part can be called a one-way large-size part, for which separate deposition and subsequent welding or gluing together of the parts are possibly the most common and feasible solutions. However, during the FDM process, the deposition-induced effect may be remarkable, particularly for some deposition materials, which can drastically improve the mechanical properties of the FDM part (Ref 29-31). Even if there is no induction effect, the deposition orientation of the part also greatly affects its mechanical strength (Ref 32-36). The method of separate deposition and subsequent welding or gluing fails to take advantage of these effects, and the fabricated parts can show inferior mechanical properties.

To effectively utilize the deposition-induced and/or deposition-oriented effect, a one-step deposition is necessary to improve the mechanical properties of the parts. In our previous studies, a continuous-printing method for one-way large-sized FDM parts was proposed (Ref 37). The fundamental running processes of the experimental FDM device are shown in Fig. 2(a-d), which present only two blocks of the printing table as an example. The main frame of the FDM machine is actually similar to the conventional one. The main difference is that the printing table of the proposed device is composed of several foldable blocks, and the driving device of every block of the printing table is installed on another movable frame. Hence, the printing table and its frame are scalable, and the

This invited article is part of a special topical focus in the *Journal of Materials Engineering and Performance* on Additive Manufacturing. The issue was organized by Dr. William Frazier, Pilgrim Consulting, LLC; Mr. Rick Russell, NASA; Dr. Yan Lu, NIST; Dr. Brandon D. Ribic, America Makes; and Caroline Vail, NSWC Carderock.

Ying-Guo Zhou and **Xiao Huang**, School of Materials Science and Engineering, Jiangsu University of Science and Technology, Zhenjiang 212003 Jiangsu, People's Republic of China. Contact e-mail: zhouyingguo@gmail.com.

scalability depends on the size of the printing parts. Once the two blocks of the printing table are combined, there is no longer any gap which may affect the surface quality of the printed parts between them. Compared with the conventional FDM machine, which can move in three directions, the continuous printer can move in the normal three directions and in addition make large steps by a defined offset, moving in x -direction from one printing bed to another. It means that the print nozzle can move in the X and Y directions, and the printing table can move in the X and Z directions. The procedure of the proposed printing method is described as follows. When a one-way large-sized sample is printed, the printer nozzle moves similarly to a conventional printer, as shown in Fig. 2(a). However, once the printer nozzle moves to the edge of the printing bed (Fig. 2b, or a designated location), the printer nozzle is elevated, and the printing is paused. Then, the elevated nozzle and printer bed simultaneously move back, as shown in Fig. 2(c). The nozzle is dropped and moved forward again, the materials are deposited on another block of the printing table, as shown in Fig. 2(d), and the printing resumes. During this process, there is a time interval during which the printer nozzle moves backward, which is very difficult to eliminate completely. The effect of the interval time on the continuous-printing process remains unknown. In addition, the linking-up location caused by the paused deposition probably affects the part quality. In this study, we focus on the issue of continuous printing and further verify the necessity and feasibility of the proposed method. An optimized method to control the printing table is suggested accordingly.

2. Experimental

2.1 Materials and Feedstock Filament Fabrication

The FDM process supports a wide variety of modeling materials. For example, polycarbonate (PC), acrylonitrile-butadiene-styrene (ABS), and (PLA). In our previous study (Ref 31), the balance between bonding properties and ductility, which can be adjusted by controlling the compatibility and porosity, was found to be an important factor to improve the

tensile behaviors of blended PC/ABS FDM parts. In this study, the blends were selected to be a represent to investigate the effect of continuous printing. A composite of PC, ABS, and ethylene-methyl acrylate copolymer (EMA) with a weight ratio of 19:19:2 was used as the experimental material. The PC [Lexan 141R, MFI 12.0 g/10 min (573 K, 21.6 N)], ABS [PA-757, MFI2.0 g/10 min (463 K, 21.6 N)], and EMA [AX8900, MFI 6 g/10 min (463 K, 21.6 N)] were commercial products. All materials were used as received and subsequently dried, weighed, and mixed by a high-speed mixer. Then, the obtained PC/ABS composite was extruded using a single-screw extruder with a single-orifice die ($\Phi 3$ mm). A moderate draw ratio (the ratio of the rolling rate to the extrudate rate) of 4.5 was used, and $\Phi 1.75$ mm feedstock filaments were fabricated. The main processing parameters of the PC/ABS/EMA feedstock filament extrusion are listed in Table 1.

2.2 FDM Sample Preparation

After the feedstock filament was prepared, it was used to directly fabricate FDM parts. The printing was controlled by the G-codes, which was revised manually based on the auto-generated codes by the open-source slicer software (Slice3r). The revision can meet the requirement of the printing route. To investigate and evaluate the mechanical properties of the FDM parts in a facile manner, fully solid samples prepared with the printing route in Fig. 3(a) were first printed using the conventional FDM method, and the results are shown in Fig. 3(e). The selective processing parameters of the FDM process are listed in Table 2.

To compare the conventional FDM method with the proposed method, an FDM sample was separately prepared and glued together. Its deposition route is shown in Fig. 3(b), and the sample is shown in Fig. 3(f). The FDM sample of continuous printing was prepared using the method in Fig. 2(a-d) according to the printing route in Fig. 3(c), and the sample is shown in Fig. 3(g). Figure 3(g) shows that there is an accumulation of materials in the middle of the sample, which can be attributed to the interval time, which leads to the outflow of the melted filament and depends on the running speed of the FDM machine. To eliminate the effect of the interval time on the shape of the FDM parts, the printing route was optimized

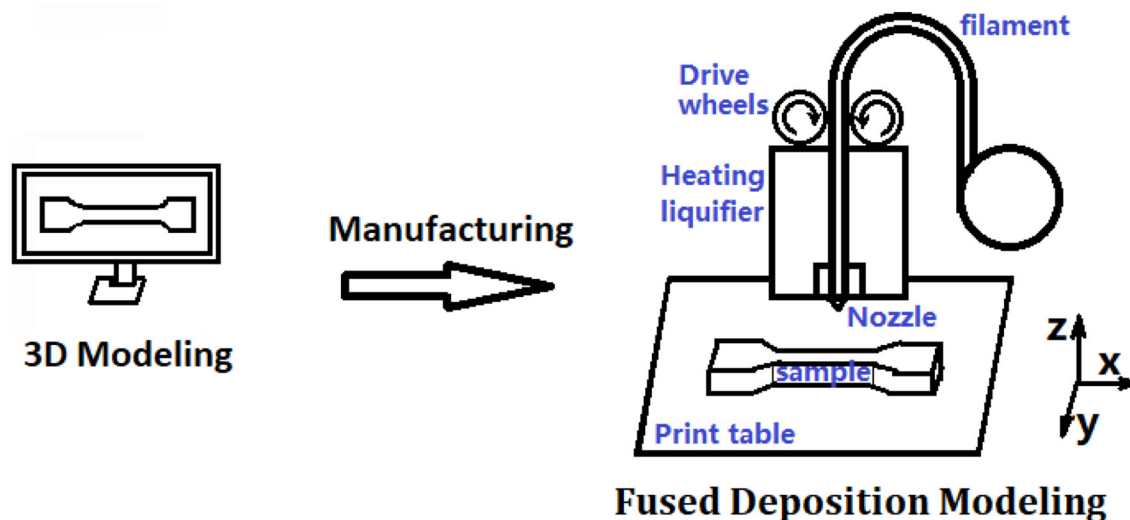


Fig. 1 Sketched description of basic FDM process

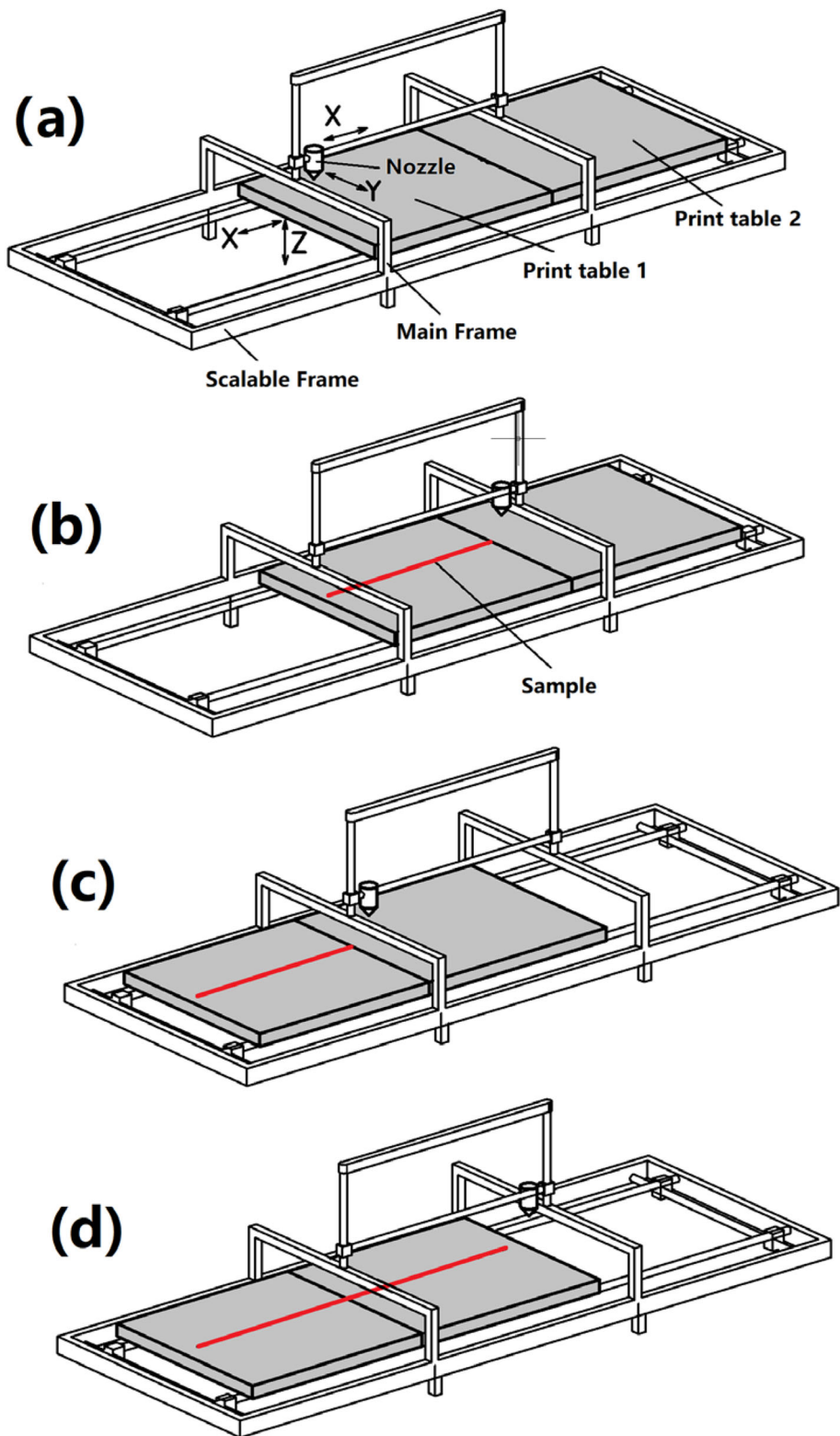


Fig. 2 Sketched description of fundamental printing procedures (a-d) to print one-way large-size parts

and is shown in Fig. 3(d). In this process, the printer nozzle is not returned to a known position at the edge of the printing table but is moved into an adjacent zone of the edge of the printing table. Using the adjusted printing route, the FDM

sample was fabricated using the interval times of 300 and 160 ms, and the shapes are shown in Fig. 3(h).

In addition, Fig. 3(g) shows that the materials accumulated. An interval time of 240 ms is common for a 200 mm wide

printing table. To investigate the effect of the interval time on the mechanical properties of the FDM parts, a series of experiments was performed, and the results are shown in Fig. 4 and 5. The optimized result of the tensile test is shown in Fig. 6.

2.3 Characterization

Tensile tests were performed on a screw-driven universal testing instrument (MTS, Sintech 10/GL) using a constant crosshead speed of 10 mm/min. At least seven tensile bars were tested for each group, and the mean and range of the tensile strength and strain-at-break for each test sample were calculated.

The morphologies of the manufactured specimens were examined using scanning electron microscopy (SEM JEOL JSM-5000). The SEM specimens were taken from the cross section at the assigned location of the printed tensile bar, which was a tensile fractured surface or fractured in liquid nitrogen depending on the observed location. To make the samples electrically conductive, the surfaces of the selective surface were sputter-coated with a thin gold layer prior to observation.

Table 1 Main processing parameters of the filament extrusion

Parameter	Value
Temperature of nozzle, °C	220-240 K
Speed of screw rotation, rpm	120
Speed of take-up rolls, m/s	0.58
Temperature of take-up rolls, °C	50

3. Results and Discussion

3.1 Necessity and Feasibility of Continuous Printing

The necessity of continuous printing can be first proven by a direct comparison of mechanical properties between the conventional FDM and the continuous-printed FDM samples. Compared with the stress-strain behavior of the conventional FDM sample (Fig. 4a), that of the sample whose parts were separately printed and glued together shows obvious brittle fractures (Fig. 4b). The strain-at-break value of the sample is only approximately 5%, which is much lower than that of the conventional FDM sample, which shows a ductile fracture with a strain-at-break of 30%. The tensile strength (35 MPa) of the glued FDM sample is also obviously lower than that of the conventional FDM sample (50 MPa). In addition, the locations of fracture of the two samples vary. The conventional FDM sample flexibly and randomly fractured in the gauge section, as shown in Fig. 7(a). However, the glued sample only ruptured in the sticky position, as shown in Fig. 7(b), which indicates that

Table 2 Main processing parameters of the FDM process

Parameter	Value
Nozzle temperature, °C	250
Deposition speed, mm/h	2000
Temperature of printing table, °C	95
Layer thickness, mm	0.2

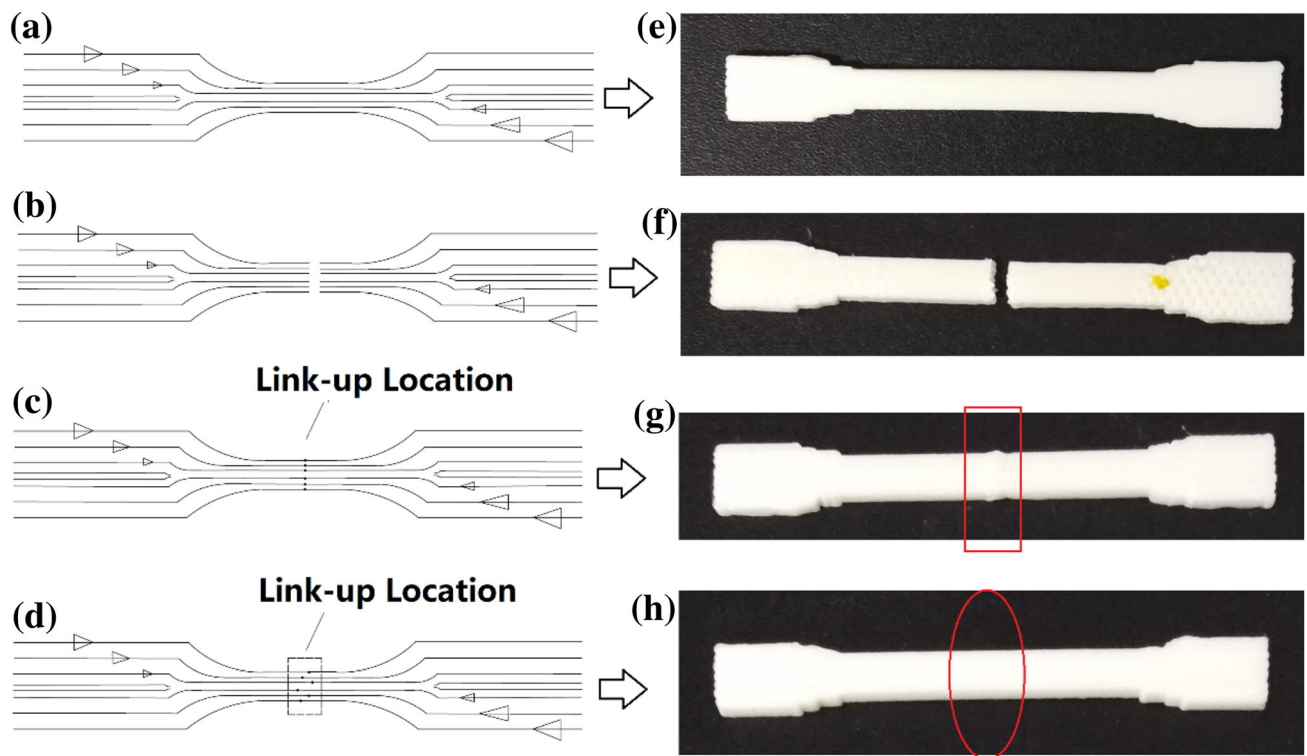
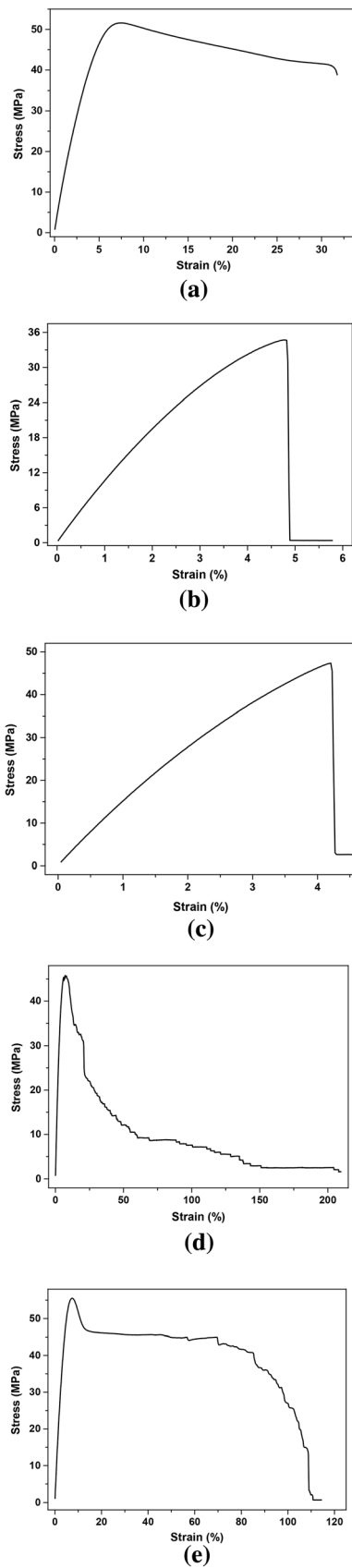


Fig. 3 Experimental results of the FDM process (a-d: printing path, e, f: original printed samples; a and e: conventional FDM printed; b and f: separately printed and glued; c and g: continuous-printed with the same linking-up locations; d and h: continuous printed with different linking-up locations)



◀ **Fig. 4** Stress–strain curves of the FDM samples (a: conventional FDM sample; b: separately printed and glued sample; c: continuous-printed with the same linking-up locations; d: continuous printed with different linking-up locations and an interval time of 240 ms; e: continuous printed with different linking-up locations and an interval time of 160 ms)

only the glued location contributes to the weak mechanical properties of the samples. Furthermore, compared with that of the regularly prepared surface of the conventional FDM sample, which was fractured in liquid nitrogen, as shown in Fig. 7(a), the morphology of the fracture surface of the glued sample in Fig. 7(b) shows that the adhesive coating is strongly bonded, which indicates that the fracture zone in Fig. 7(b) was well adhered due to the function of the glue. Nonetheless, the glued location remains weaker than other deposited locations. This result is expected considering that the stretching effect of printed polymer materials in the FDM process produces a certain orientation, which can improve the mechanical properties of the printed parts. Hence, continuous printing is necessary to improve the mechanical properties of one-way large-sized FDM parts.

After the continuous-printed sample (Fig. 7c) was fabricated using the methods mentioned in Fig. 1 and 2, the necessity of these methods can be proven once again by comparing the mechanical properties. For convenience of comparison, the size and shape of the continuous FDM sample, except for the printing path, were identical to those of the conventional FDM sample. Because the sample was repeatedly deposited on two blocks of printer tables, fully consistent with the proposed ideas of continuous printing, the continuous FDM sample is considered. The tensile test results of the continuous sample in Fig. 4(c) show that although the continuous-printed sample also shows an obvious brittle fracture and a strain-at-break as low as 5%, the tensile strength, which is 45 MPa, is higher than that of the glued sample in Fig. 4(b). Thus, the high tensile properties of the continuous-printed sample compared to those of the glued sample indicate that continuous printing is necessary and feasible.

As mentioned, the deposited polymer possibly flows outward when the printer nozzle moves backward, which results in an accumulation of materials (circled in Fig. 3g) as observed from the shape of the FDM sample. In addition, the site of accumulation may be a weakness of the whole sample. Hence, the fractured locations of the continuous-printed sample are found to be the connection point of the adjacent printing table, as shown in Fig. 7(c). Interestingly, the morphology of the fracture surface includes two parts: the normally printed part (marked in the box) and the accumulated materials, as shown in Fig. 7(c).

Because the interval time cannot be avoided in the proposed method of continuous printing, it is an important factor of the mechanical properties of the FDM parts and must be clarified.

3.2 Effect of the Interval Time on the Continuous-Printed Part

Figure 5 shows the effect of the interval time on the tensile strength of the continuous-printed parts, and Fig. 6 shows the stress–strain curves of five representative samples. At least, 120 ms are necessary for the nozzle to move backward stably. Figure 5 shows that the tensile strength exhibits a trend of

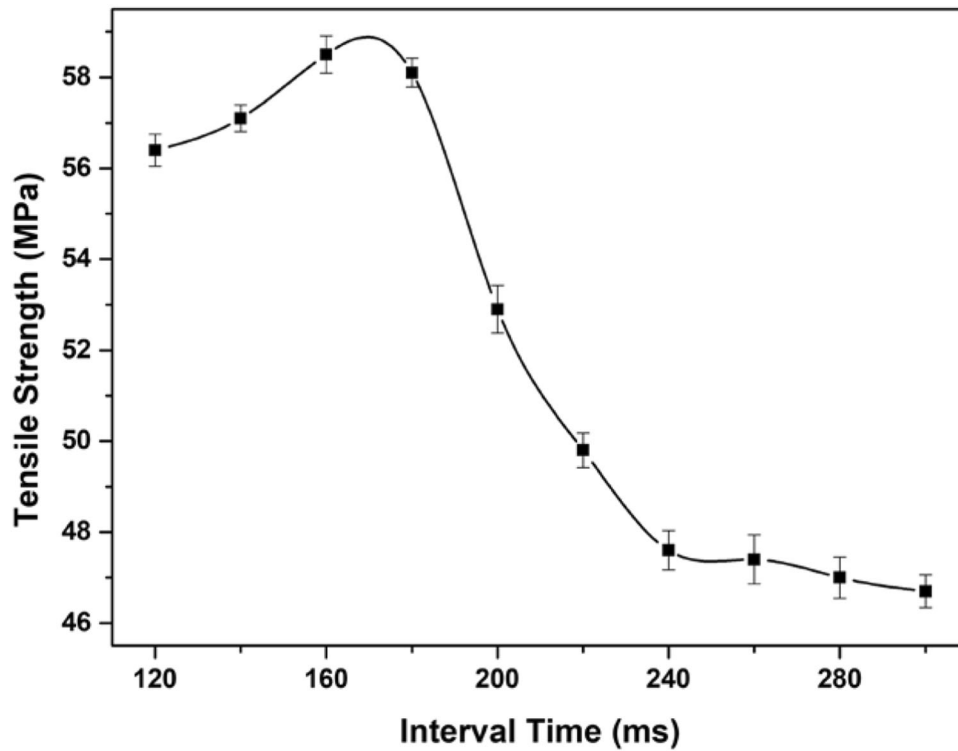


Fig. 5 Effect of the interval time on the tensile strength of the continuous printed sample

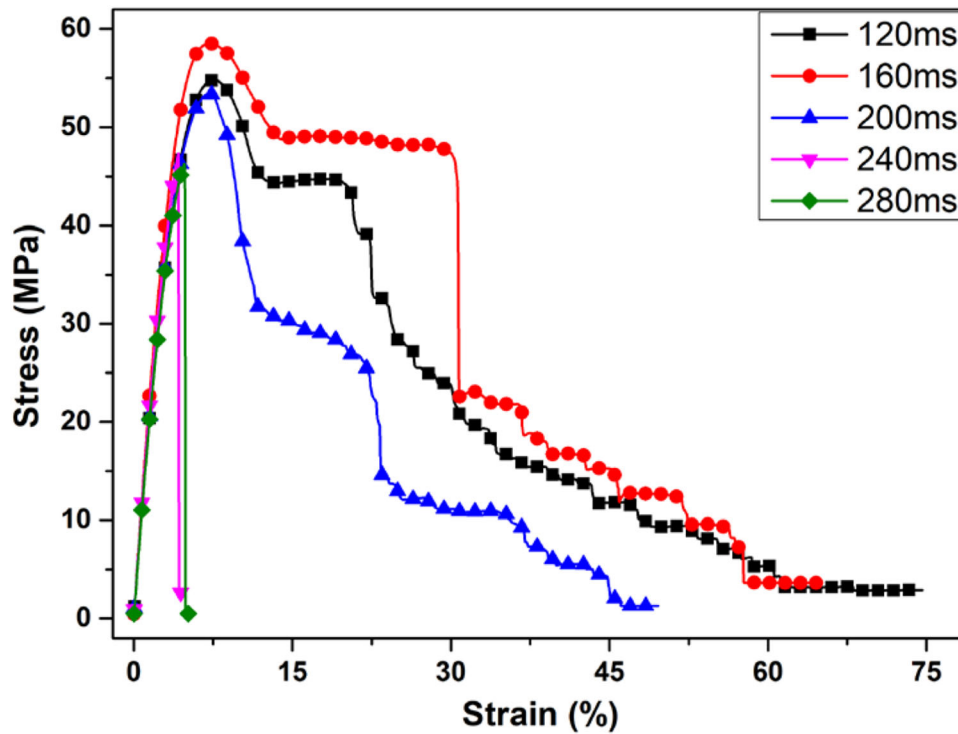


Fig. 6 Stress–strain curves of the continuous-printed sample with different interval times

gentle increase and drastic decrease with increasing interval time. Overall, a short interval time is beneficial for improving the mechanical properties, which can be observed from the stress–strain behavior in Fig. 6. The fracture behavior in the

tensile test can be obviously separated into two types: brittle and tough. When the interval time exceeds 200 ms, the fracture behavior is obviously brittle, as observed in Fig. 4(c). However, if the interval time is less than 200 ms, the samples are tough,

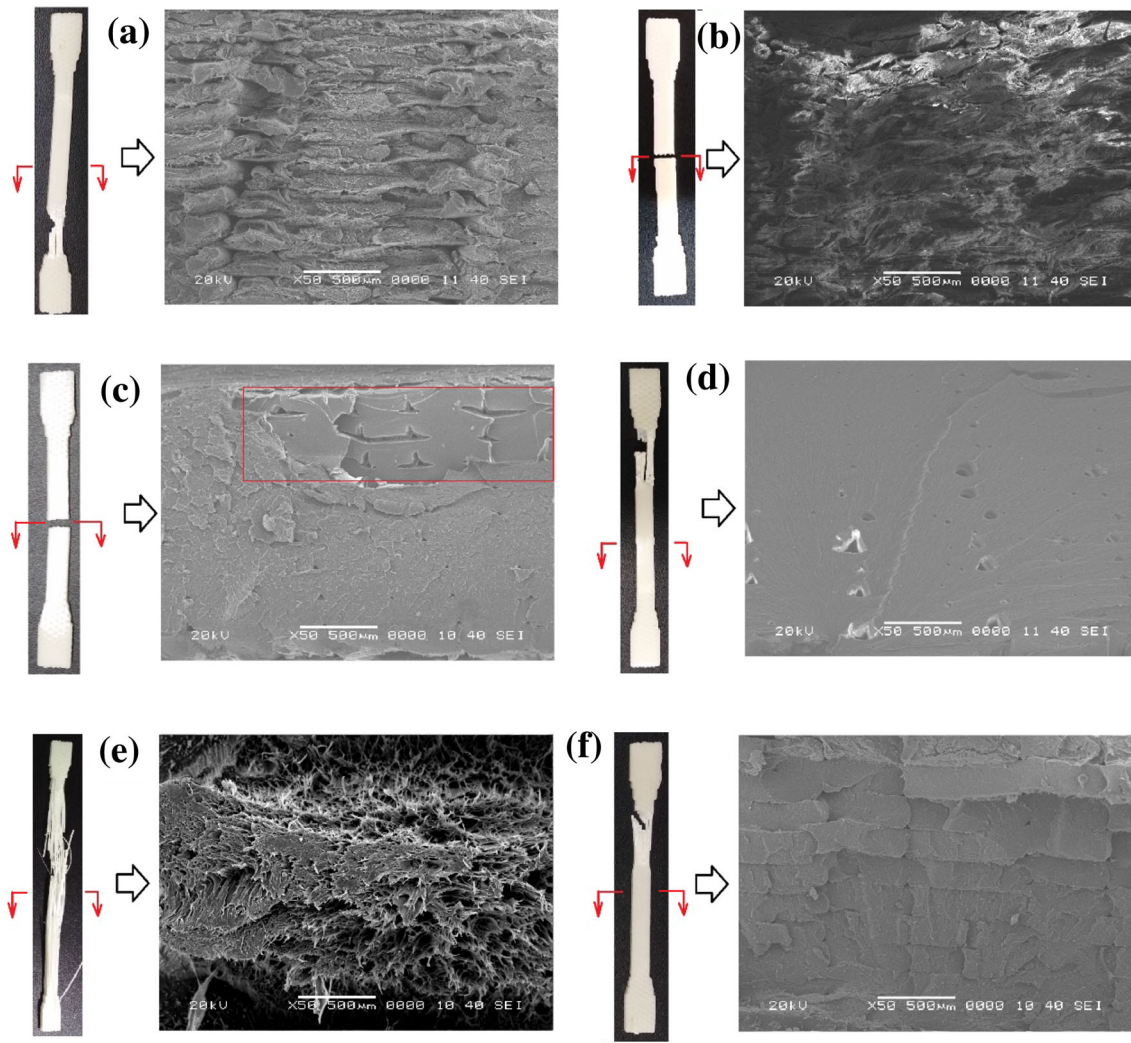


Fig. 7 Tested samples and their SEM images (a: conventional FDM processed; b: separately printed and glued; c: continuous-printed with the same linking-up locations; d: continuous-printed sample with an optimized interval time of 160 ms; e: continuous printed with different linking-up locations and an interval time of 240 ms; f: continuous printed with different linking-up locations and an interval time of 160 ms)

and the strain-at-break exceeds 10%. For a short interval time of less than 160 ms, the decrease in mechanical properties can be attributed to the fast movement, which may cause the FDM machines to vibrate slightly and result in unstable printing. Therefore, an interval time of 120-200 ms is permitted in the FDM processes, which guarantees the feasibility of the presented method continuous printing. The effect of the interval time on the mechanical properties also reflects the importance of continuous printing by showing that continuous printing helps to ensure that adequate mechanical properties are achieved.

To further illustrate the tough fracture behavior, Fig. 7(d) shows a continuous-printed sample with an interval time of 160 ms. Here, the sample did not fracture at the site of material accumulation, which indicates that the latter is no longer the weakness of the sample. Therefore, the negative effect of the interval time can be eliminated by optimization. Furthermore, compared to those in the accumulation location in Fig. 7(d), the deposited materials in the accumulation location in Fig. 7(d) are better fused and distributed. This result is consistent with the ductile fracture behavior of the sample. Thus, the feasibility of continuous printing is proven again.

However, the shape of the continuous-printed sample shown in Fig. 7(d) still indicates an accumulation location in the materials. The application of the FDM process can be altered depending on the appearance of the sample. Eliminating the accumulation location by optimizing the printing route is necessary, as discussed below.

3.3 Optimization of the Linking-Up Location

In previous continuous-printing methods, the nozzle is always moved back when the printing proceeds to the edge of a block of printing table. Hence, all switching points are located on a line. During the interval time, the flow of the melted filament causes the material to accumulate. Hence, controlling the location of the nozzle to randomly move back in an adjacent zone of the edge of the printer table is a reasonable solution. The printing route is shown in Fig. 3(d), and the fabricated sample is shown in Fig. 3(h). Figure 3(h) shows that hardly any of the materials accumulated, and the shape of the fabricated continuous-printed sample is almost identical to that of the conventional FDM sample. This similarity is attributed to the homogenization of the small amount of outflow materials at

different locations of the switching point in the FDM process. The fracture behavior of the sample in Fig. 4(d) is different from the results in Fig. 4(c) and obviously shows ductility. Hence, the mechanical properties are improved using the optimized deposition route. However, the sample cannot be considered perfect. The gauge section of the tensile sample is separated into bunches of fibers during the tensile test, as shown in Fig. 7(e). Hence, although the nominal strain-at-break is higher than that of the conventional FDM sample, the total absorbance work (area under the stress–strain curve) remains lower.

The effects of the interval time on the mechanical properties are proved again by a comparison between the stress–strain plots of the optimized continuous-printing process and those with a different interval time. When the interval time is shortened to 160 ms, the stress–strain curves and appearance of the sample (Fig. 4e, 7f, respectively) show that the sample has better mechanical behavior than that of the sample in Fig. 7(e). Thus, compared to those of all previously discussed samples, the tensile behaviors of the samples in Fig. 7(f) may be the most suitable for practical applications, although many also have high nominal tensile strength and strain-at-break values. The necking of the sample can spread far in the tensile process, which indicates that the deposited filaments can uniformly bear the load under the tensile test. The good mechanical response can be attributed to the tightly ordered deposition structure, which can be reflected by the perfect cross-sectional morphology in Fig. 7(f). Compared to the structure of the cross section of the conventional sample in Fig. 7(a), that of the deposited filament of the sample in Fig. 7(f) shows a close stacking to withstand strong stresses and deformation. Therefore, the results show that optimizing the interval time and linking-up location is an efficient method to fabricate one-way large-sized FDM parts with high mechanical properties. Thus, the necessity and feasibility of the continuous-printing method are proven accordingly. This method also serves as a template and guide for printing multiway large-sized parts. In addition, for a real FDM application, the printing paths are usually complex. However, regardless of complexity, a similar procedure can be achieved using the proposed method. The automatic method of modifying the controlling code of the continuous printer will be further reported separately. It is also possibly that the interval time is avoided completely in further study. In addition, theoretically, as long as a material can be used in the FDM process, it has the potential to be used in the continuous printing process. Further investigation of the feasibility of this method and mechanisms for other polymers and their blends/composites is underway.

4. Conclusion

In this study, a method for the continuous printing of one-way large-sized FDM parts was proposed, and the necessity and feasibility of the method were investigated via a comparison of the stress–strain behavior, fracture characteristics, and microstructural morphology among FDM samples fabricated using different printing processes. Thus, the continuous printing of one-way large-size FDM parts is very important. Continuous printing is also feasible because of an allowed interval time. Furthermore, the method in this study is efficient for continuous printing; in particular, the interval time and

linking-up location were optimized, and the method is therefore worth applying and popularizing.

Acknowledgments

The authors would like to express their gratitude to the Jiangsu Province Industry–University–Research Project (BY2020380) and the Postgraduate Research and Practice Innovation Program of Jiangsu Province (Grant No. KYCX20_3130) for their financial support.

Conflict of interest

The authors state that there is no conflict of interest.

References

1. B.N. Turner, R. Strong and S.A. Gold, A Review of Melt Extrusion Additive Manufacturing Processes I. Process Design and Modeling, *Rapid Prototyp. J.*, 2014, **20**(3), p 192–204
2. S.S. Banerjee, S. Burbine, and N.K. Shivaprakash, 3D-Printable PP/SEBS Thermoplastic Elastomeric Blends: Preparation and Properties, *Polymers*, 2019, **11**(2), p 347
3. P. Parandoush, C. Zhou, and D. Lin, 3D Printing of Ultrahigh Strength Continuous Carbon Fiber Composites, *Adv. Eng. Mater.*, 2019, **21**(2), p 1800622
4. T. Feuerbach, S. Callau-Mendoza, and M. Thommes, Development of Filaments for Fused Deposition Modeling 3D Printing with Medical Grade Poly(Lactic-Co-Glycolic Acid) Copolymers, *Pharm. Dev. Technol.*, 2019, **24**(4), p 487–493
5. E.R. Fitzharris, D.W. Rosen, and M.L. Shofner, Fast Scanning Calorimetry for Semicrystalline Polymers in Fused Deposition Modeling, *Polymer*, 2019, **166**, p 196–205
6. O.A. Mohamed, S.H. Masood, J.L. Bhowmik, M. Nikzad, and J. Azadmanjiri, Effect of Process Parameters on Dynamic Mechanical Performance of FDM PC/ABS Printed Parts Through Design of Experiment, *J. Mater. Eng. Perform.*, 2016, **25**(7), p 2922–2935
7. M. Jin, R. Giesa, C. Neuber, and H.W. Schmidt, Filament Materials Screening for FDM 3D Printing by Means of Injection-Molded Short Rods, *Macromol. Mater. Eng.*, 2018, **303**, p 1800507
8. D.A. Anderegg, H.A. Bryant, and D.C. Ruffin, In-Situ Monitoring of Polymer Flow Temperature and Pressure in Extrusion Based Additive Manufacturing, *Addit. Manuf.*, 2019, **26**, p 76–83
9. I. Durgun and R. Ertan, Experimental Investigation of FDM Process for Improvement of Mechanical Properties and Production Cost, *Rapid Prototyp. J.*, 2014, **20**(3), p 228–235
10. D.A. Roberson, A.R. Torrado Perez, C.M. Shemely, A. Rivera, and R.B. Wicker, Comparison of Stress Concentrator Fabrication for 3D printed Polymeric Izod Impact Test Specimens, *Addit. Manuf.*, 2015, **7**, p 1–11
11. C.C. Kuo, Y.R. Wu, and M.H. Li, Minimizing Warpage of ABS Prototypes Built with Low-Cost Fused Deposition Modeling Machine Using Developed Closed-Chamber and Optimal Process Parameters, *Int. J. Adv. Manuf. Technol.*, 2019, **101**(1–4), p 593–602
12. L.P. Bressan, C.B. Adamo, and R.F. Quero, A Simple Procedure to Produce FDM-Based 3D-Printed Microfluidic Devices with an Integrated PMMA Optical Window, *Anal. Methods*, 2019, **11**(8), p 1014–1020
13. O.A. Mohamed, S.H. Masood, and J.L. Bhowmik, Experimental Investigation of Time-Dependent Mechanical Properties of PC-ABS Prototypes Processed by FDM Additive Manufacturing Process, *Mater. Lett.*, 2017, **193**, p 58–62
14. C. Cassavola, A. Cazzato, and V. Moramarco, Mechanical Behaviour of ABS-Fused Filament Fabrication Compounds under Impact Tensile Loadings, *Materials*, 2019, **12**(8), p 1295
15. Q. Li, W. Zhao, Y. Li, W. Yang, and G. Wang, Flexural Properties and Fracture Behavior of CF/PEEK in Orthogonal Building Orientation by FDM: Microstructure and Mechanism, *Polymers*, 2019, **11**(4), p 656

16. C. Bellehumeur, L. Li, Q. Sun, and P. Gu, Modeling of Bond Formation Between Polymer Filaments in the Fused Deposition Modeling Process, *J. Manuf. Process.*, 2004, **6**(2), p 170–178
17. U.K.U. Zaman, E. Boesch, and A. Siadat, Impact of Fused Deposition Modeling (FDM) Process Parameters on Strength of Built Parts Using Taguchi's Design of Experiments, *Int. J. Adv. Manuf. Technol.*, 2019, **101**(5–8), p 1215–1226
18. S. Jiang, G. Liao, and D. Xu, Mechanical Properties Analysis of Polyetherimide Parts Fabricated by Fused Deposition Modeling, *High Perform. Polym.*, 2019, **31**(1), p 97–106
19. S.N. Cerda-Avila, H.I. Medellin-Castillo, and D.F. De lange, Analysis and Numerical Simulation of the Structural Performance of Fused Deposition Modeling Samples With Variable Infill Values, *J. Eng. Mater. Technol.-Trans. ASME*, 2019, **141**(2), p 021005
20. H. Xia, J. Lu, and G. Tryggvason, A Numerical Study of the Effect of Viscoelastic Stresses in Fused Filament Fabrication, *Comput. Methods Appl. Mech. Eng.*, 2019, **346**, p 242–259
21. J.J. Zhang, P. Wang, and R.X. Gao, Deep Learning-Based Tensile Strength Prediction in Fused Deposition Modeling, *Computes in Industry*, 2019, **107**, p 11–21
22. S.R. Rajpurohit and H.K. Dave, Analysis of Tensile Strength of a Fused Filament Fabricated PLA Part Using an Open-Source 3D Printer, *Int. J. Adv. Manuf. Technol.*, 2019, **101**(5–8), p 1525–1536
23. K. Ilyes, N.K. Kovacs, and A. Balogh, The Applicability of Pharmaceutical Polymeric Blends for the Fused Deposition Modelling (FDM) 3D Technique: Material Considerations-Printability-Process Modulation, with Consecutive Effects on In Vitro Release, Stability and Degradation, *European Journal of Pharmaceutical Science*, 2019, **129**, p 110–123
24. Z. Viskadourakis, G. Perrakis, and E. Symeou, Transport Properties of 3D Printed Polymer Nanocomposites for Potential Thermoelectric Applications, *Appl. Phys. A Mater. Sci. Process.*, 2019, **125**(3), p 159
25. D. Douroumis, 3D Printing of Pharmaceutical and Medical Applications: a New Era, *Pharm. Res.*, 2019, **36**(3), p UNSP42
26. A.J. Capel, R.P. Rimington, and J.W. Fleming, Scalable 3D Printed Molds for Human Tissue Engineered Skeletal Muscle, *Front. Bioeng. Biotechnol.*, 2019, **7**, p 20
27. M. Revilla-Leon and M. Ozcan, Additive Manufacturing Technologies Used for Processing Polymers: Current Status and Potential Application in Prosthetic Dentistry, *J. Prosthodont. Implant Esthet. Reconstr. Dent.*, 2019, **28**(2), p 146–158
28. S. Masood, Advances in Fused Deposition Modeling, in Hashmi S. *Comprehensive Materials Processing*. Elsevier Ltd. 2014, vol. 10, p 69–91
29. Y.G. Zhou, B. Su, and L.S. Turng, Depositing- Induced Effects of Isotactic Polypropylene and Polycarbonate Composites During Fused Deposition Modeling, *Rapid Prototyp. J.*, 2017, **23**(5), p 869–880
30. B. Su, Y.G. Zhou, and H.H. Wu, Influence of Mechanical Properties of PP/LDPE Nanocomposites: Compatibility and Crystallization, *Nanomater. Nanotechnol.*, 2017, **7**, p 1–11
31. Y.G. Zhou, J.R. Zou, H.H. Wu, and B.P. Xu, Balance Between Bonding and Deposition during Fused Deposition Modeling of Polycarbonate and Acrylonitrile-Butadiene-Styrene Composites, *Polym. Compos.*, 2020, **41**(1), p 60–72
32. S.H. Ahn, M. Montero, D. Odell, S. Roundry, and P.K. Wright, Anisotropic Material Properties of Fused Deposition Modeling ABS, *Rapid Prototyp. J.*, 2002, **7**(4), p 248–257
33. K. Thrimurthulu, P.M. Pandey, and N.V. Reddy, Optimum Part Deposition Orientation in Fused Deposition Modeling, *Int. J. Mach. Tools Manuf.*, 2004, **44**, p 585–594
34. Y.G. Zhou, B. Su, and L.S. Turng, Mechanical Properties, Fiber Orientation, and Length Distribution of Glass Fiber-Reinforced Polypropylene Parts: Influence of Water-Foaming Technology, *Polym. Compos.*, 2018, **39**, p 4386–4399
35. H. Liu, H. He, and X. Peng, Three-Dimensional Printing of Poly(Lactic Acid) Bio-Based Composites with Sugarcane Bagasse Fiber: Effect of Printing Orientation on Tensile Performance, *Polym. Adv. Technol.*, 2019, **30**(4), p 910–922
36. J.F. ParreiraLovo, C.A. Fortulan, and M.M. Da Silva, Optimal Deposition Orientation in Fused Deposition Modeling for Maximizing the Strength of Three-Dimensional Printed Truss-Like Structures, *Proc. Inst. Mech. Eng. Part B J. Eng. Manuf.*, 2019, **233**(4), p 1206–1215
37. Y.G. Zhou, J.J. Zhou, and Y.X. Mei, Fabrication Method of One-Way Large-sized Fused Deposition Modeled Parts and Its Printing Equipment. *Chinese Patent*, ZL 201611074949.1, 2018-09-29

Publisher's Note Springer Nature remains neutral with regard to jurisdictional claims in published maps and institutional affiliations.